IEEE Access
Multidisciplinary | Rapid Review | Open Access Journal

Received May 22, 2019, accepted June 10, 2019, date of publication July 8, 2019, date of current version August 12, 2019.

Digital Object Identifier 10.1109/ACCESS.2019.2927402

Dahlin-Based Fast and Robust Current Control of a PMSM in Case of Low Carrier Ratio

STEFAN WALZ[1], (Student Member, IEEE), RADU LAZAR[2], (Member, IEEE), GIAMPAOLO BUTICCHI[3], (Senior Member, IEEE), AND MARCO LISERRE[1], (Fellow, IEEE)

[1]Chair of Power Electronics, University of Kiel, 24143 Kiel, Germany
[2]Danfoss Silicon Power, 6300 Gråsten, Denmark
[3]Zhejiang Key Laboratory on the More Electric Aircraft Technologies, University of Nottingham Ningbo China, Ningbo 315100, China

Corresponding author: Giampaolo Buticchi (buticchi@ieee.org)

This work was supported in part by the European Union/Interreg V-A—Germany–Denmark, through the PE:Region Project, and in part by the Ningbo Science and Technology Beauro under Grant 2018A-08-C.

ABSTRACT The low ratio of sampling frequency to electrical frequency (carrier ratio) is a challenging issue for applications, such as high-speed or high-power drives. In fact, high-speed drives have high fundamental frequency and high-power drives have low switching (sampling) frequency, leading to the same control challenges of having high dynamic and stability with a limited number of control actions in one period. Parameters mismatch occurs due to the converter non-linearities, deadtimes, temperature change, and saturation; hence, providing robust control is a key challenge. This paper starts reviewing the problems of controlling machines with a few switching instances per fundamental period and an analysis of the state-of-the-art current control strategies for permanent magnet synchronous motors (PMSMs). Three different control schemes are analyzed. The discrete-time PI current controller is providing good robustness, while the dynamic performance may not be sufficient for some applications. Second, the deadbeat control offers very fast dynamic performance but is weak under parameter mismatch. The novel application of the Dahlin controller offers a tradeoff between performance and stability. The control algorithms are evaluated based on the stability, robustness, and dynamic and steady-state performances. Their performance and sensitivity to parameter variation are analyzed through simulations, and the experimental measurements are proving the results.

INDEX TERMS Dahlin control, deadbeat control, pulse ratio, electric drive, PMSM, current control, pulse-width modulated power converter.

The growing research interest in high-speed machines can be observed by the high number of publications in this research area. Rising attention is given to topics related to the hardware for motor drive systems with high-speed machines, such as the machine itself, the converter, the motor filters, as well as research related to the software, i.e. the control or observer design [1]–[4]. For many applications like pumps, fans, or automotive, high-speed machines are becoming more and more popular [5]. Machines up to speed of one Million r/min or a rated power of one Gigawatt are available today [2], [6]. The permanent magnet synchronous machine is the first choice for many applications due to its compact size, high power density and good efficiency.

The associate editor coordinating the review of this manuscript and approving it for publication was Ton Do.

Having a cascaded control, the performance of the current control determines the performance of the overall control system. Therefore high bandwidth, fast dynamic response, and good steady-state performance for high-frequency PMSM current control are ongoing interesting research topics.

Many approaches to control permanent magnet synchronous machines have been studied. The V/f-Control is a well-known concept and is shown to work for high-speed motors in [7]. However, this method does not control the stator currents, which can lead to deviations in the stator flux, produce torque ripple and worsen the accuracy and dynamic performance of the machine. The cascaded PI based current control with overlaid speed or torque control is common in industry and offers good steady-state performance. Advanced decoupling schemes [8] improve the dynamic performance. Also, the direct design in the discrete

time domain, the Discrete-Time Current Controller, proves to give good results for field-oriented as well as voltage oriented control [9]–[11]. These approaches offer good robustness, but the dynamic performance is not satisfying for some applications. Considerable research attention is given to predictive control. Using model predictive control, the cost function can be used to optimize performance, losses, or increase robustness, but raises high computational requirements [12]. On the other hand, the well known Deadbeat Control can be used to null the control error after a predefined number of switching periods. To be properly tuned, an exact discrete machine model is required. Due to non-linearities, parameter variation, or other mismatches, the robustness of the Deadbeat Control can be critical. Due to the very good dynamic performance, the Deadbeat Control is popular and many strategies like compensation algorithms [13], [14], observers [15]–[18], or new control systems [19], [20] are introduced and continuously adapted. The Dahlin Controller is an extension of the Deadbeat Controller and well known for controlling deadtime processes. The novel application of the Dahlin algorithm for machine control combines fast dynamic and steady-state performance, and robustness by introducing a tunable integral behavior.

The paper is organized into six sections. An overview about the challenges of controlling machines with low f_S/f_{el} ratio is given in Section I. In Section II, state-of-the-art current control strategies are compared and in Section III the Dahlin Control is introduced. The dynamic performance and effects of parameter uncertainties on the system are evaluated by simulations in Section IV. The simulation results of the evaluated control schemes are verified by experiments in Section V. Conclusions are finally drawn in Section VI.

I. OVERVIEW ON CHALLENGES OF LOW f_s/f_{el} RATIO

For electrical drive applications, the field-oriented control (FOC) with a cascaded speed (or torque) and current regulator is used in industry since many years. For high-speed drives, the rated electrical frequency of the machine can reach very high values. On the other hand, for medium to high power drives, the switching frequency f_{sw} has to be kept low. For a medium power system, a maximum switching frequency of approximately 5kHz is often used in industry, while the electrical frequency f_{el} can go up to several hundred Hertz. The decreasing ratio f_S/f_{el} can be used as characteristic value to analyze the stability of the control system. Especially at low ratios of $f_S/f_{el} < 10$, it is important to have a high current control bandwidth.

Due to the small number of switchings per fundamental period, it is also important to limit the losses in the machine and keep the total harmonic distortion of the current (THDi) below a certain value. The natural filtering due to the machine inductances is often insufficient to keep the THDi below 5%, which is often required in industry. Hence, special sinus output filters (LC-Filter) to reduce the current and voltage harmonics are required. Thus, the system gets larger, more expensive, and more complex to control [21].

Rare-earth magnets like neodymium-iron-bore (NdFeB), which are used for the permanent magnets of the rotor, are very sensitive to temperature. The rotor temperature has to be kept strictly below a defined temperature, to prevent irreversible demagnetization of the magnets. In literature, there are many ways to estimate or monitor the rotor temperature, e.g. presented in [22]. In high performance drives high control bandwidth and accuracy is required. Deviations can lead to distortion of the stator flux linkage [10]. The resulting torque ripples can harm the mechanical parts of the system, like the machine, gearbox, or mechanical coupling.

II. CURRENT CONTROL STRATEGIES

The analyzed current control strategies in this paper are using modulators and are therefore easy to compare, as they can be interchanged without changes in the control structure. A switching frequency of 1kHz is chosen and DSP provides the calculation power for the use of asymmetrical PWM. Using double update PWM, the delay due to the PWM could be halved, from one switching period to $T_{d,PWM} = 0.5\ T_{sw}$. Multisampling strategies can help to reduce the delay further, thus, increasing the bandwidth and improving the control response [23]. For the use of DSP and direct design of the controllers in the discrete time domain, equation (1) shows the dependency of the digital system from the sampling time, the first-order differential term between two sampling periods can be approximated.

$$\frac{d}{dt}i(t) = \frac{i(k+1) - i(k)}{T_S} \tag{1}$$

Fig. 1 shows the control scheme of the considered system. The voltage source converter (VSC) is controlled by a cascaded control structure with speed and subordinated current control and it provides a voltage of variable amplitude and frequency to the permanent magnet synchronous machine (PMSM). Equation (2) shows the continuous-time state-space representation of the PMSM, where the stator current i_S is chosen as state variable and the inputs are the stator voltage v_S and PM flux Ψ_{PM}. Pulse width modulation is used to realize the voltage space vectors.

$$\frac{d\boldsymbol{i}_s(t)}{dt} = \boldsymbol{A}_m\boldsymbol{i}_s(t) + \boldsymbol{B}_m\boldsymbol{v}_s(t) + \boldsymbol{c}_m\Psi_{PM} \tag{2}$$

$$\boldsymbol{A}_m = \begin{bmatrix} -R_s/L_d & \omega_{el}L_q/L_d \\ -\omega_{el}L_d/L_q & -R_s/L_q \end{bmatrix}$$

$$\boldsymbol{B}_m = \begin{bmatrix} \frac{1}{L_d} & 0 \\ 0 & \frac{1}{L_q} \end{bmatrix}$$

$$\boldsymbol{c}_m = \begin{bmatrix} 0 \\ -\omega_{el}/L_q \end{bmatrix} \tag{3}$$

A. DISCRETIZED PI CONTROL

The PI control is well-known for controlling electrical machines in industry [24]. The most common method to

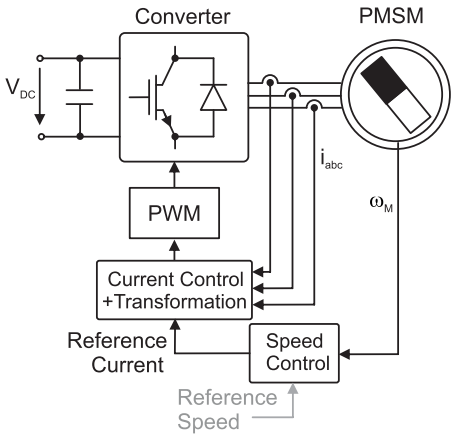

FIGURE 1. Schematic of control scheme with Converter, Control, and PMSM.

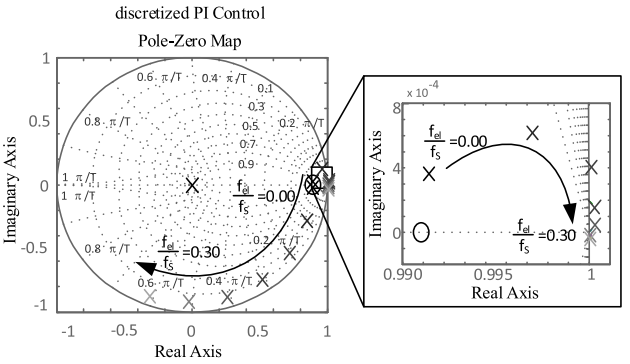

FIGURE 2. Pole-Zero map of Discretized PI Control for $f_{el}/f_S = [0.00, 0.05, \ldots, 0.30]$.

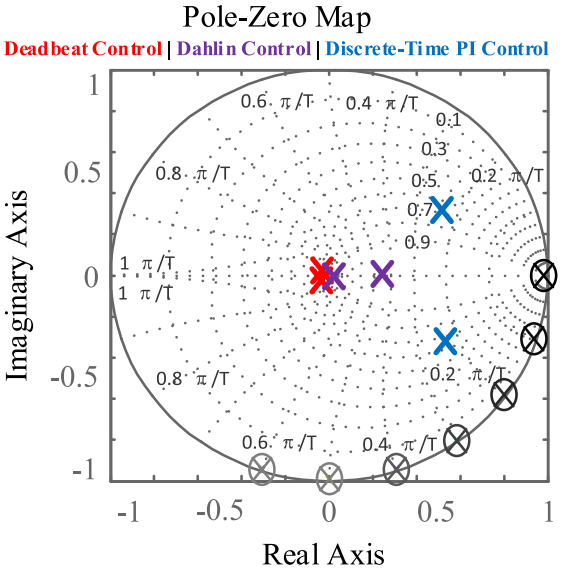

FIGURE 3. Pole-Zero map of Deadbeat Control (red), Dahlin Control (purple), and Discrete-Time PI Control (blue) for $f_{el}/f_S = [0.00, 0.05, \ldots, 0.30]$.

design a PI controller for digital systems is to perform the design in the continuous time domain and then use the Euler Methods to transfer the controller into the discrete time domain. The discrete time representation of the PI controller with a proportional and an integral part is defined as

$$G_{PI}(s) = K_P + \frac{K_I}{s} \tag{4}$$

Equation (5) shows the discretized transfer function using Tustin transformation.

$$G_{PI}(z) = G_{PI}(s)\Big|_{s=\frac{2}{T_S}\frac{z-1}{z+1}} = K_P + \frac{K_I T_S}{2}\frac{z+1}{z-1} \tag{5}$$

For example, in [11] an approach to tune the PI controller depending on the desired bandwidth is shown. In equations (6) and (7) with L' and R' defined as the nominal values at zero speed, while ω_0 defines the required bandwidth.

$$K_P = L' \cdot \omega_0 \tag{6}$$

$$K_I = R' \cdot \omega_0 \tag{7}$$

For rising fundamental to switching frequency the pole zero map of the discretized PI controller is shown in Fig. 2. At small ratio, where conventional machines are usually operated, the PI controller provides good results, but for rising ratios, the controller becomes instable. Fig. 2 shows the pole-zero map of the control. At a frequency of $f_{el}/f_S \approx 0.07$, the poles drift out of the unit circle and the control gets unstable. To overcome these problems, many methods like the State Feedback Decoupling or delay compensations have been introduced. This way, the performance of the controller can be improved, but it is not possible, to eliminate the time dependency of the controller [10].

B. DIRECT DESIGN OF A DISCRETE TIME DOMAIN CURRENT CONTROLLER

A possibility to overcome the frequency dependent instability in the discrete time domain is to design directly in the discrete time domain (Discrete-Time PI Control) [9]. The discrete transfer functions are obtained by using a zero-order hold voltage latch.

$$G_{P,dq}(z) = \frac{i_d(z)}{v_d(z)} = \frac{z-1}{z}\mathcal{Z}\left\{\mathcal{L}^{-1}\left\{\frac{G_{P,dq}(s)}{s}\right\}\right\} \tag{8}$$

Based on the discretized plant model, the PI controller is tuned to cancel the time dependent pole of the plant. $K_{PI,dd}$ can be used to define the dynamic response of the controller.

$$G_{\mathrm{PI,dd}}(z) = K_{\mathrm{PI,dd}} \cdot \frac{z - z_0}{z - 1} \tag{9}$$

Fig. 3 (blue) shows the pole-zero map of the closed loop controller, including the time dependent pole-zero-cancellation. As the PI Controller is very well known, this strategy is easy to adapt and implement. The dynamic performance is still good, with a rise time of three sampling periods and a settling time of seven sampling periods. However, depending on the application it can be beneficial to have faster dynamic response.

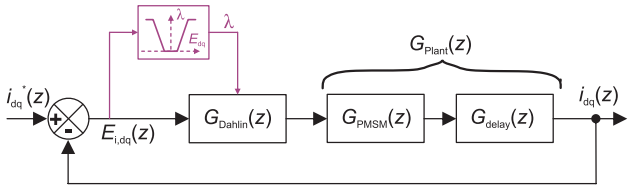

FIGURE 4. Block scheme of the Dahlin control system.

C. DEADBEAT CONTROL

The Deadbeat Control is well known and is given increasing attention for the control of motor-tied applications in the last years. Many different designs of Deadbeat control have been presented in literature, focusing on time delay compensation, robustness, or many other [13].

The idea of the Deadbeat Control is to null the error after a given number of sampling periods. Taking into account the calculation and sampling time, it can be seen, that a minimum of two sampling periods is required for the Deadbeat control.

$$G_{\text{Deadbeat}}(z) = \frac{1}{G_{\text{Plant}}(z)} \cdot \frac{z^{-2}}{1 - z^{-2}} \tag{10}$$

The Deadbeat Control algorithm requires a good knowledge of the electrical machine model and their parameter values. The processing and calculation period takes one sampling period. As shown in equations (11) and (12), the PWM voltages can be calculated based on the predicted currents and the output voltages based on the sampled values and are applied at the (k+2)-th period. The measured values in the k-th period are used for the calculations the (k+1)-th period and $i_{dq}^*(k)$ are used as the reference currents.

$$v_d(k+1) = \frac{L_d}{T_S}\left(i_d^*(k) - i_d(k+1)\right) + R_s i_d(k+1) - L_q \omega_{el} i_q(k+1) \tag{11}$$

$$v_q(k+1) = \frac{L_q}{T_S}\left(i_q^*(k) - i_q(k+1)\right) + R_s i_q(k+1) + L_d \omega_{el} i_d(k+1) + \omega_{el}\Psi_{PM} \tag{12}$$

The closed loop pole-zero-map is shown in Fig. 3 (red). As shown in equation (10), the controller compensates the system dynamics completely, if the system parameters are well known. This makes the Deadbeat Control susceptible to parameter variations. Using the wrong parameters, not compensating the temperature dependent rise of the motor resistances, or the saturation of the inductances can lead to undesirable results. The dynamic performance worsens and overshoots or oscillation may occur, which lead to torque ripple. In addition, the steady-state performance can suffer and lead to a steady-state control error.

III. DAHLIN CONTROL

The Dahlin Control is based on the Deadbeat Controller and extends the Deadbeat Control with an integral behavior. While the Deadbeat Control has a very fast dynamic performance but lacks under parameter variation, the Discrete-Time

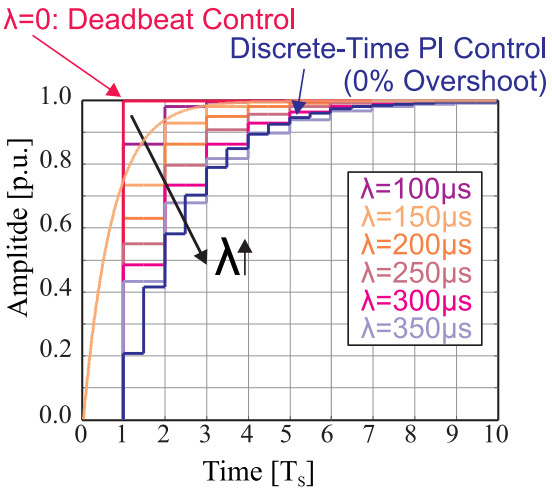

FIGURE 5. Closed loop Dahlin Control Step response for $\lambda = [0, 100\,\mu s, 150\,\mu s, \ldots, 350\,\mu s]$.

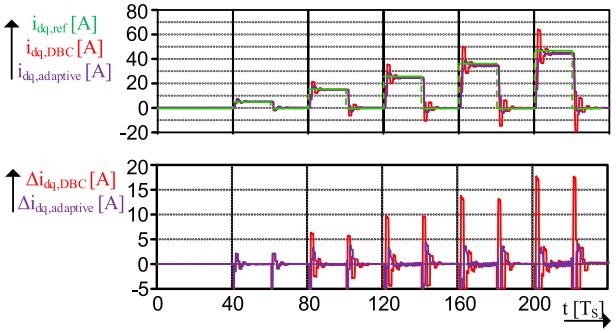

FIGURE 6. Comparison of Deadbeat Control (red) and adaptive Dahlin Control (purple): Increasing Current reference steps [5A, 15A, . . . , 45] and step responses (top), and current error (bottom).

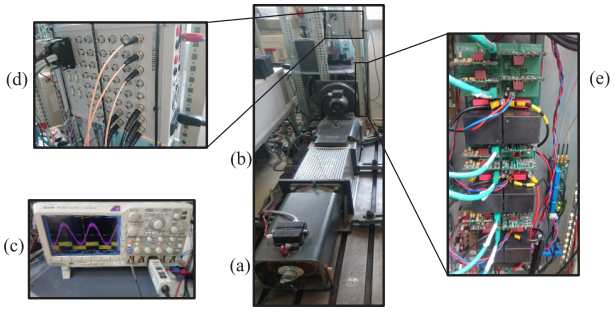

FIGURE 7. Experimental setup: (a) Siemens PMSM, (b) DC Load machine, (c) Oscilloscope, (d) DSpace MicroLabBox, (e) Converter.

PI Control has a good stability and steady-state performance, but the dynamic performance needs to be improved for some applications. With the Dahlin controller, a trade-off can be chosen, which is easy to implement, robust, fast, and has a good performance. The control structure was introduced by E.B. Dahlin in 1968 and is a digital controller [25], used for processes with deadtimes [26], [27]. By extending the Deadbeat Control with the integral part, model mismatches like parameter changes, system non-linearities, and saturation

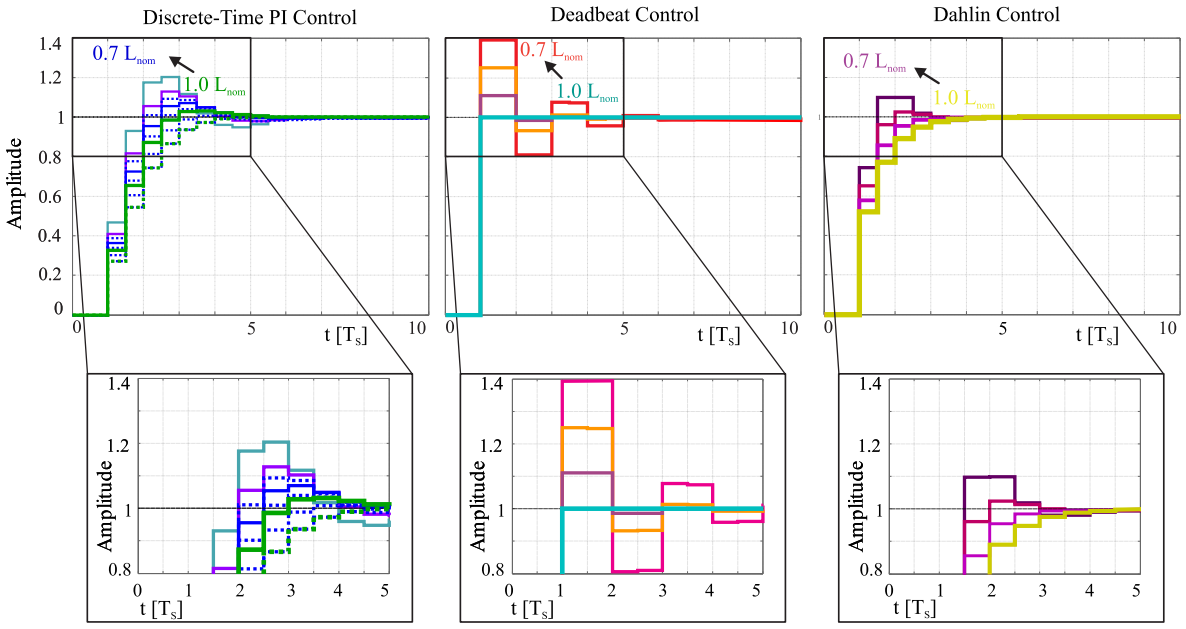

FIGURE 8. Step response: Discrete-Time PI Control (solid: 3% Overshoot; dotted: No Overshoot) with varied/nominal parameters: blue/green; Deadbeat Control with varied/nominal parameters: red/turquoise; Dahlin Control ($\lambda = 100\mu s$) with varied/nominal parameters: purple/yellow.

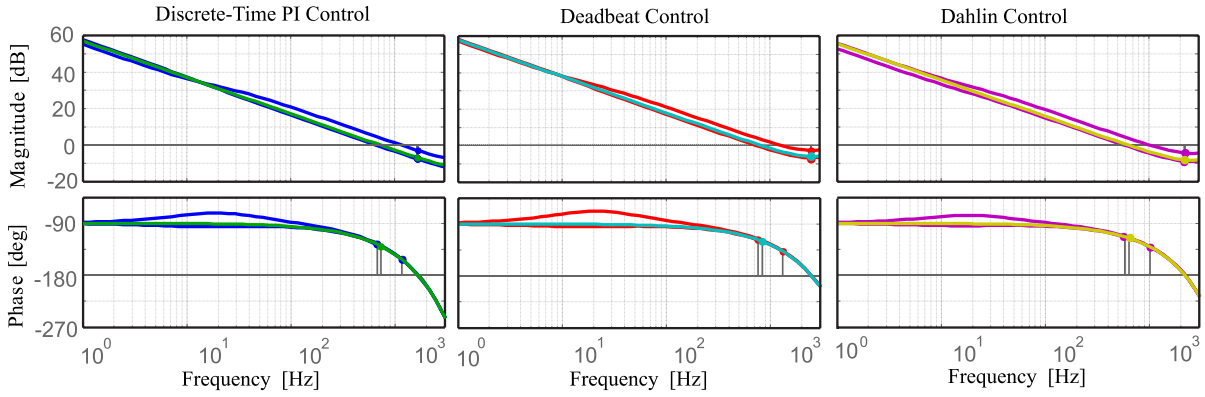

FIGURE 9. Bode plot open loop current control strategies: Discrete-Time PI Control (3% Overshoot) with varied/nominal parameters: blue/green; Deadbeat Control with varied/nominal parameters: red/turquoise; Dahlin Control with varied/nominal parameters: purple/yellow.

effects can be compensated. Equations (13) and (14) show the design of the controller.

$$G_{\text{Dahlin}}(z) = \frac{1}{G_{\text{Plant}}(z)} \cdot \frac{T(z)}{1 - T(z)} \tag{13}$$

$$T(z) = \frac{\left(1 - e^{-\frac{T_S}{\lambda}}\right) \cdot z^{-2}}{1 - e^{-\frac{T_S}{\lambda}} \cdot z^{-2}} = \frac{(1-\alpha) \cdot z^{-2}}{1 - \alpha \cdot z^{-2}} \tag{14}$$

The parameter λ is used as a tuning factor and defines the behavior of the control. For $\lambda = 0$, the Dahlin Control is identical to the Deadbeat Control. For $\lambda > 0$, the continuous response is defined by the ratio of time constant λ and the sampling time T_S in the numerator, $(1 - e^{-\frac{T_S}{\lambda}})$. This can be solved to set the rise time T_{rise}, defined as the time to rise from 10% to 90%, and settling time T_{settling}, the time for the response to reach and stay within a 2% error band of its final value, of the control. An exemplary waveform is shown in Fig. 5 (orange).

$$T_{\text{rise}} = 2.2 \cdot \frac{\lambda}{T_S}, \quad T_{\text{settling}} = 4 \cdot \frac{\lambda}{T_S} \tag{15}$$

The pole-zero-map of the closed loop control using the Dahlin Controller is shown in Fig. 3 (purple). While one pole is still in the origin, the second pole is depended on the tuning parameter λ. In addition, there is pole-zero-cancellation of the frequency dependent poles.

Using the Dahlin Control, a trade-off between fast dynamic performance and high robustness can be chosen and, at the same time, keeping good steady-state performance. The tuning factor λ can be used to adapt the control to the required

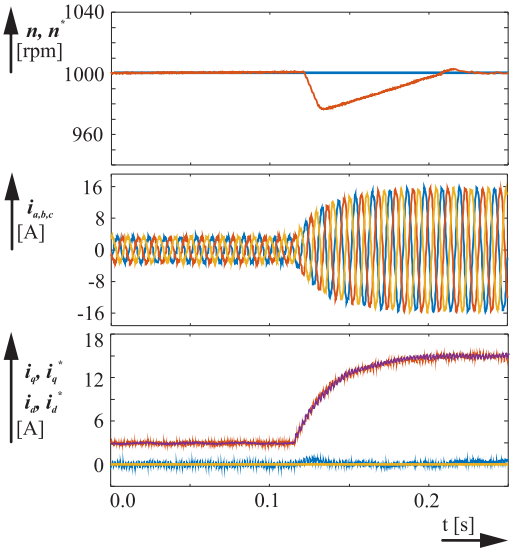

FIGURE 10. Dahlin Control: Load step at nominal speed ($f_{el} = 100\ Hz$), $f_S = f_{sw} = 1000\ Hz$; top: speed (red) and reference speed (blue), middle: phase current $i_{a,b,c}$, bottom: i_d (blue), $i_{d,ref}$ (yellow), i_q (red), $i_{q,ref}$ (purple).

system and desired performance or even changed online, as shown in Section IV. The control structure of the Dahlin Current Control in the discrete time domain is shown in Fig. 4, where $G_{\text{Dahlin}}(z)$ is the Dahlin Controller, eq. (13), $G_{\text{PMSM}}(z)$ the transfer function of the machine, eq. (11) and (12), and $G_{\text{delay}}(z)$ the two period delay. The effect of the tuning parameter λ (also rewritten as unit-free value α) are analyzed in Fig. 5. For $\lambda = 0$, the Dahlin Controller is equal to the Deadbeat Controller (turquoise). With increasing time constant λ, the integrational part of the Dahlin Controller is becoming more important and the rise time increases. Choosing a time constant of $\lambda = 350\mu s$, the settling time is equal to the settling time of the Discrete-Time PI Controller, thus, depending on the parameters of the machines and the application, the tuning parameter lambda should be chosen between $\lambda = [0, 350\mu s]$.

IV. SIMULATION RESULTS

A. ROBUSTNESS ANALYSIS

To analyze and compare the performance of the current controllers, MATLAB Robust Control Toolbox is used. To take the saturation of the inductances into account, the nominal inductances are varied in the range of $70\% - 100\%\ L_{nom}$. The heating of the motor increases the motor resistance, which increases the damping and therefore improves the stability. Hence, it does not have to be considered in a worst-case scenario.

For the dynamic analysis, the step responses for varied parameters are shown in FIGURE 8. The Discrete-Time PI Controller (blue) shows higher oscillation and variance of the rise and settling time. While the nominal overshoot is only 3%, at worst case the overshoot can rise up to 20%. Using a more robust design without overshoot (0%, dotted lines), the Discrete-Time PI Control shows the most robust behavior

TABLE 1. Machine setup data.

$P_{\text{PMSM,rated}}$	22kW
n_{rated}	2000rpm
f_{el}	100Hz
pole pairs	3
$L_{\text{s,dq}}$	2.2μH
R_{s}	0.1Ω

TABLE 2. Converter setup data.

V_{DC}	560V
f_{sw}	1kHz
T_{deadtime}	2μs

in regards to phase and gain margin, but the dynamic performance worsens and the rise and settling times rise. Also the Deadbeat Controller faces an overshoot. While using nominal values the error can be nulled after two sampling periods and without overshoot, worst case behavior shows an overshoot of 20% and a steady-state error. The Dahlin Control shows the least deviation due to the parameter variation. Using a λ-factor of $100\mu s$, the nominal settling time of three sampling periods is only slightly higher than for the Deadbeat Control and only a small overshoot occurs. With varied parameters, the settling time can rise, but only a very small overshoot occurs.

To increase the robustness, λ could also be changed online. λ of the Dahlin Control is changed depending on the absolute value of the current error in a defined range, for example like given in Fig. 5, and can be added as input to the control, Fig. 4 (purple). In Fig. 6 simulation results for reference current steps are shown. For small changes in the reference current, a very fast response is preferable. In case the motor inductances are saturated or other parameter variation occur, the relative overshoot is high, but the absolute overshoot of the current can be handled by the system. On the other hand, if the changes in the reference current are high, an increasing λ-factor is desirable. This way, under nominal parameters the torque reference can be limited, reducing the mechanical stress, and, in case of parameters variations, the over-current is reduced. Also more advanced ways of adapting λ are possible, e.g. based on model reference as shown in [28] or on the observed disturbance [29].

The Bode plot of the open-loop transfer function is shown in FIGURE 9. The nominal inductances are varied in the range of $70\% - 105\%\ L_{nom}$ and the stator resistance between $90\% - 200\%\ R_{nom}$. While the Dahlin Control shows the best results for the phase and gain margin, all three controllers prove their high bandwidth even under worst-case parameter variation. The results are summarized in Table 3 and Table 4.

V. EXPERIMENTAL RESULTS

The simulation results of the current controllers are validated by experiments with a 22kW *Siemens PMSM*, connected

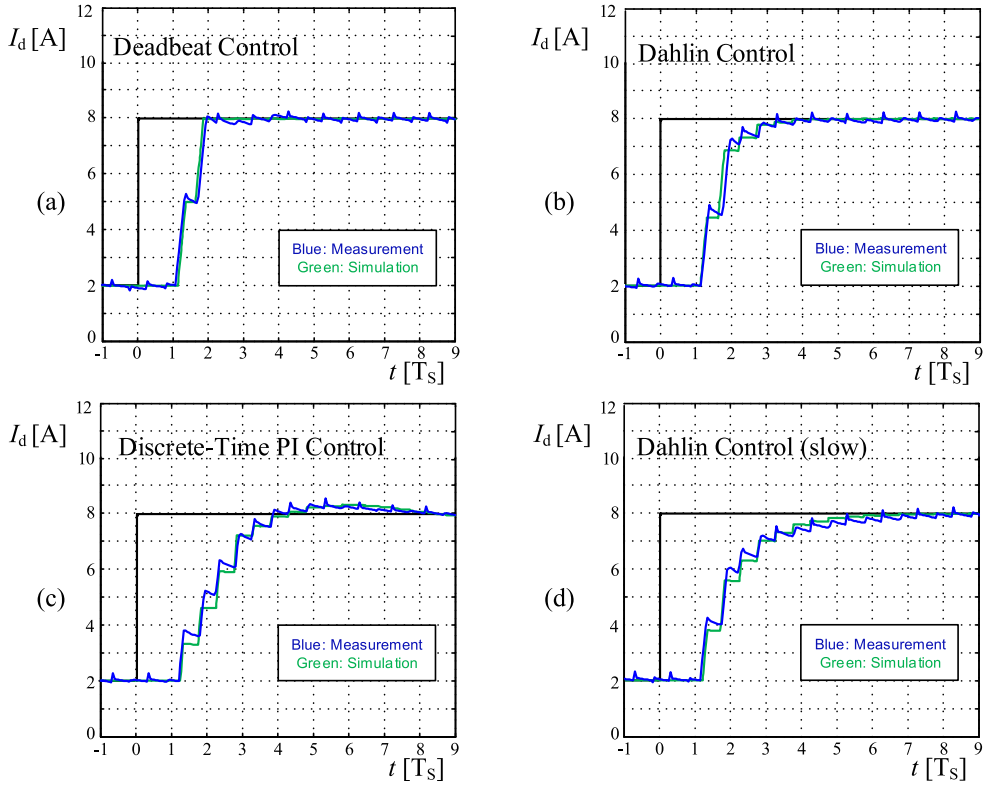

FIGURE 11. Performance for measured and simulated step response: (a) Deadbeat Control, (b) Dahlin control ($\lambda = 100\,\mu s$), (c) Discrete-Time PI Control, (d) slow Dahlin Control ($\lambda = 250\,\mu s$).

to a DC load machine. The DC link of the converter is connected to a 20kW DC voltage source. The waveform of the output current is measured and recorded by a *Tektronix DPO3014 Oscilloscope* with a *Tektronix TCP0030* Current Probe. The inductance and resistance of the machine were measured with a *Sourcetronic ST2826A LCR meter* and are given in Table 1, the operation point of the converters is listed in Table 3. No additional motor-filters are used. A *DSpace MicroLabBox* is used to control the system. The laboratory setup is shown FIGURE 7.

A. NOMINAL OPERATION

In FIGURE 10 the Dahlin control is tested with a load step at nominal speed and a carrier ratio of $f_S/f_{el} = 10$ is shown. As it can be seen, the speed controller works correctly, increasing the q-component of the current.

As the decoupled current dynamics for d-/ and q-current are equal, the step response for a 6A d-component current reference step from $i_d = 2A$ to $i_d = 8A$ at stand-still is chosen to validate the performance of the controllers and avoid unwanted torque effects. Additionally, the rotor is locked to provide similar initial conditions for all test cases. The voltage drop of the semiconductors and the deadtime are compensated for this operation point. The results are shown in FIGURE 11.

The experimental results prove the simulation results. Under nominal conditions, the Deadbeat control nulls the error after two switching period, FIGURE 11 (a). In addition, the successful tuning of the Dahlin Control is proven. In FIGURE 11 (b) the fast dynamic response (with $\lambda = 100\mu s$) is comparable to the Deadbeat Control and the integrational behavior can be seen. Using a slower tuning ($\lambda = 250\mu s$) in FIGURE 11 (d), the settling time is similar to the Discrete-Time PI Current Control, but no overshoot occurs, which can be beneficial to avoid over-current and consequential torque ripples can be avoided.

B. OPERATION UNDER PARAMETER VARIATION

To test the robustness of the control strategies, the control parameters are increased to simulate the saturation of the inductances and are measured in five operation points for $L_{s,dq} = [100\%, \ldots, 60\%]$. Under parameter variation, the simulated behavior, shown in Section IV, could be proven. The slightly lower overshoots can occur due to increased motor resistance R_s and consequently higher damping. As shown in FIGURE 12(a), the expected very fast rise time of the Deadbeat Control comes with the drawback of the biggest overshoot under saturation. FIGURE 12(b) shows the measured step responses of the Dahlin Controllers with a small time constant λ ($\lambda = 100\mu s$). In this way, the step response is smoothened while the overshoot under parameter variation is reduced. Compared to the Deadbeat Control, the rise time increases by one sampling period T_S.

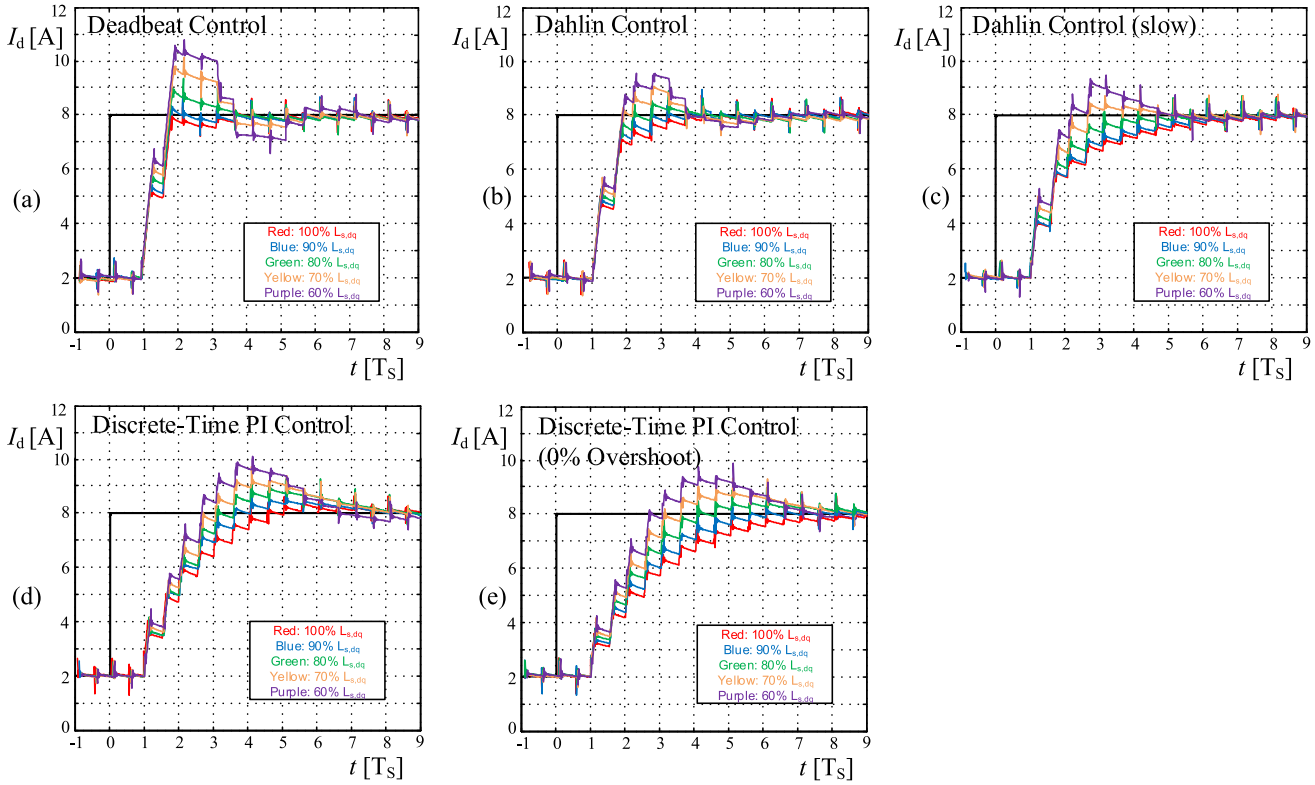

FIGURE 12. Measured Current Step Response Performance under parameter variation ($L_{s,dq} = [100\%, \ldots, 60\%]$): (a) Deadbeat Control, (b) Dahlin control ($\lambda = 100\,\mu s$), (c) Discrete-Time PI Control, (d) slow Dahlin Control ($\lambda = 250\,\mu s$).

TABLE 3. Performance comparison of current control strategies.

	Rise time [T_S]	Settling time [T_S]	Perc. Overshoot	No steady-state error
Discrete-Time PI Control	3	6	3%	√
Deadbeat Control	2	2	0%	X
Dahlin Control	3	3	0%	√

TABLE 4. Robustness analysis for current control strategies.

	Phase margin			Gain margin [dB]			Crossover Frequency [Hz]		
	MIN	NOM	MAX	MIN	NOM	MAX	MIN	NOM	MAX
Discrete-Time PI Control									
3% Overshoot	39.1°	53.7°	57.4°	4.17	6.70	7.53	675	728	756
0% Overshoot	54.6°	65.0°	67.5°	7.65	10.7	11.0	439	464	666
Deadbeat Control	46.7°	60.0°	62.9°	3.21	6.02	6.84	752	834	1210
Dahlin Control	49.4°	64.6°	66.7°	4.59	8.24	9.05	575	632	1020

In FIGURE 12(d), the measured results of the Discrete-Time PI Current Control are shown. The results are compared to the Dahlin Controller tuned to have the same settling time in nominal operation point, but without an overshoot ($\lambda = 250\mu s$). While the Discrete-Time PI Current Control has a maximum overshoot of approximately 40% with a 30% saturation of the inductances, the Dahlin Controller shows higher robustness. Also tuning the Discrete-Time PI Control to have no Overshoot in nominal operation point, FIGURE 12(e), the rise and settling times increase, while the sensitivity to the parameter variation is higher than for the Dahlin Controller.

VI. CONCLUSION

In this paper, modulator based current control strategies for permanent magnet synchronous motors with low ratios of sampling to electrical frequency are compared. The well-known Deadbeat Control and direct designed PI Control are compared with the novel application of the Dahlin

Controller. Especially for low ratios of f_S/f_{el} the controllers are pushed to their limits and high robustness to parameter variations is required. The detailed robustness analysis shows good behavior for all current control strategies, whereas the Dahlin Controller shows also very good dynamic and steady-state performance for high parameter variation. The experimental results prove the analyzed behavior. While all investigated control strategies are stable, the Dahlin Controller offers a good solution to increase the robustness of the closed loop control system. Under worst case parameter variation, the maximum overshoot can be reduced by approximately 20 percentage points compared to the Deadbeat Control and, compared to the discrete-time PI Control, the settling time can be reduced by three sampling periods. It can be concluded that the proposed control is at the same time faster than the PI and more robust than the Deadbeat to parameter variations.

REFERENCES

[1] N. Bernard, R. Missoum, L. Dang, N. Bekka, H. B. Ahmed, and M. E.-H. Zaim, "Design methodology for high-speed permanent magnet synchronous machines," *IEEE Trans. Energy Convers.*, vol. 31, no. 2, pp. 477–485, Jun. 2016.

[2] A. Borisavljevic, H. Polinder, and J. A. Ferreira, "On the speed limits of permanent-magnet machines," *IEEE Trans. Ind. Electron.*, vol. 57, no. 1, pp. 220–227, Jan. 2010.

[3] J. D. Park, C. Khalizadeh, and H. Hofmann, "Design and control of high-speed solid-rotor synchronous reluctance drive with three-phase LC filter," in *Proc. 40th IAS Annu. Meeting. Conf. Rec. Ind. Appl. Conf.*, Oct. 2005, pp. 715–722.

[4] H. Kim, J. Son, and J. Lee, "A high-speed sliding-mode observer for the sensorless speed control of a PMSM," *IEEE Trans. Ind. Electron.*, vol. 58, no. 9, pp. 4069–4077, Sep. 2011.

[5] D. Lusignani, D. Barater, G. Franceschini, G. Buticchi, M. Galea, and C. Gerada, "A high-speed electric drive for the more electric engine," in *Proc. IEEE Energy Convers. Congr. Expo. (ECCE)*, Sep. 2015, pp. 4004–4011.

[6] T. Baumgartner, R. M. Burkart, and J. W. Kolar, "Analysis and design of a 300-W 500 000-r/min slotless self-bearing permanent-magnet motor," *IEEE Trans. Ind. Electron.*, vol. 61, no. 8, pp. 4326–4336, Aug. 2014.

[7] T. Halkosaari, "Optimal U/f-control of high speed permanent magnet motors," in *Proc. IEEE Int. Symp. Ind. Electron.*, Jul. 2006, pp. 2303–2308.

[8] H. Zhu, X. Xiao, and Y. Li, "PI type dynamic decoupling control scheme for PMSM high speed operation," in *Proc. 5th Annu. IEEE Appl. Power Electron. Conf. Expo. (APEC)*, Feb. 2010, pp. 1736–1739.

[9] N. Hoffmann, F. W. Fuchs, M. P. Kazmierkowski, and D. Schröder, "Digital current control in a rotating reference frame—Part I: System modeling and the discrete time-domain current controller with improved decoupling capabilities," *IEEE Trans. Power Electron.*, vol. 31, no. 7, pp. 5290–5305, Jul. 2016.

[10] A. Altomare, A. Guagnano, F. Cupertino, and D. Naso, "Discrete-time control of high-speed salient machines," *IEEE Trans. Ind. Appl.*, vol. 52, no. 1, pp. 293–301, Jan./Feb. 2016.

[11] H. Kim, M. W. Degner, J. M. Guerrero, F. Briz, and R. D. Lorenz, "Discrete-time current regulator design for AC machine drives," *IEEE Trans. Ind. Appl.*, vol. 46, no. 4, pp. 1425–1435, Jul./Aug. 2010.

[12] W. Xie, X. Wang, F. Wang, W. Xu, R. M. Kennel, D. Gerling, and R. D. Lorenz, "Finite-control-set model predictive torque control with a deadbeat solution for PMSM drives," *IEEE Trans. Ind. Electron.*, vol. 62, no. 9, pp. 5402–5410, Sep. 2015.

[13] M. Tang, A. Gaeta, K. Ohyama, P. Zanchehtta, and G. Asher, "Assessments of dead beat current control for high speed permanent magnet synchronous motor drives," in *Proc. 9th Int. Conf. Power Electron. ECCE Asia (ICPE-ECCE Asia)*, Jun. 2015, pp. 1867–1874.

[14] P. Kakosimos and H. Abu-Rub, "Deadbeat predictive control for PMSM drives with 3-L NPC inverter accounting for saturation effects," *IEEE Trans. Emerg. Sel. Topics Power Electron.*, vol. 6, no. 4, pp. 1671–1680, Dec. 2018.

[15] X. Zhang, B. Hou, and Y. Mei, "Deadbeat predictive current control of permanent-magnet synchronous motors with stator current and disturbance observer," *IEEE Trans. Power Electron.*, vol. 32, no. 5, pp. 3818–3834, May 2017.

[16] B. Wang, Z. Dong, Y. Yu, G. Wang, and D. Xu, "Static-errorless deadbeat predictive current control using second-order sliding-mode disturbance observer for induction machine drives," *IEEE Trans. Power Electron.*, vol. 33, no. 3, pp. 2395–2403, Mar. 2018.

[17] H. Yang, Y. Zhang, J. Liang, B. Xia, P. D. Walker, and N. Zhang, "Deadbeat control based on a multipurpose disturbance observer for permanent magnet synchronous motors," *IET Electr. Power Appl.*, vol. 12, no. 5, pp. 708–716, May 2018.

[18] S. A. Davari, F. Wang, and R. M. Kennel, "Robust deadbeat control of an induction motor by stable MRAS speed and stator estimation," *IEEE Trans. Ind. Informat.*, vol. 14, no. 1, pp. 200–209, Jan. 2018.

[19] M. H. Vafaie, B. M. Dehkordi, P. Moallem, and A. Kiyoumarsi, "Improving the steady-state and transient-state performances of PMSM through an advanced deadbeat direct torque and flux control system," *IEEE Trans. Power Electron.*, vol. 32, no. 4, pp. 2964–2975, Apr. 2017.

[20] R. S. Dastgerdi, M. A. Abbasian, H. Saghafi, and M. H. Vafaie, "Performance improvement of permanent-magnet synchronous motor using a new deadbeat-direct current controller," *IEEE Trans. Power Electron.*, vol. 34, no. 4, pp. 3530–3543, Apr. 2019.

[21] K. Peter, S. Hanke, F. Mink, and J. Böcker, "Inverter loss management for an electrical high-speed drive system," in *Proc. 18th Eur. Conf. Power Electron. Appl. (EPE)*, Sep. 2016, pp. 1–10.

[22] S.-C. Carpiuc, "Rotor temperature detection in permanent magnet synchronous machine-based automotive electric traction drives," *IEEE Trans. Power Electron.*, vol. 32, no. 3, pp. 2090–2097, Mar. 2017.

[23] X. Zhang and J. W. Spencer, "Study of multisampled multilevel inverters to improve control performance," *IEEE Trans. Power Electron.*, vol. 27, no. 11, pp. 4409–4416, Nov. 2012.

[24] K.-K. Huh and R. D. Lorenz, "Discrete-time domain modeling and design for AC machine current regulation," in *Proc. IEEE Ind. Appl. Annu. Meeting*, Sep. 2007, pp. 2066–2073.

[25] E. Dahlin, "Designing and tuning digital controllers," *Instrum. Control Syst.*, vol. 41, no. 6, pp. 77–83, Jun. 1986.

[26] Y. Dong, "Stability gain interval of dahlin control system," in *Proc. 6th World Congr. Intell. Control Automat.*, Jun. 2006, pp. 486–489.

[27] Z. Zhi-Gang, Z. Ben-Guo, and B. Zhen-Fu, "Dahlin algorithm design and simulation for time-delay system," in *Proc. Chin. Control Decis. Conf.*, Jun. 2009, pp. 5819–5822.

[28] K.-H. Kim, "Model reference adaptive control-based adaptive current control scheme of a PM synchronous motor with an improved servo performance," *IET Electr. Power Appl.*, vol. 3, no. 1, p. 8, Jan. 2009.

[29] R. Yang, M.-Y. Wang, L.-Y. Li, C.-M. Zhang, and J.-L. Jiang, "Robust predictive current control with variable-gain adaptive disturbance observer for PMLSM," *IEEE Access*, vol. 6, pp. 13158–13169, 2018.

STEFAN WALZ (S'16) was born in Nuremberg, Germany, in 1987. He received the B.Sc. and M.Sc. degrees in electrical engineering and business administration from the Chistian-Albrechts-University of Kiel, Kiel, Germany, where he is currently pursuing the Ph.D. degree.

His current research interests include control of electric drives, dc–ac converter, multilevel converter, and model predictive control.

RADU LAZAR (M'14) received the M.Sc. degree in advanced electrical drives and robots from the Technical University of Cluj-Napoca and the M.Sc. degree in power electronics and drives from Aalborg University. He was with Danfoss Drives A/S, Gråsten, Denmark. His expertise is in the control of electrical machines and drives, grid connected inverters, specifically in solar and drives applications, PWM techniques, harmonic mitigation, and plant control.

GIAMPAOLO BUTICCHI (S'10–M'13–SM'17) received the master's degree in electronic engineering and the Ph.D. degree in information technologies from the University of Parma, Italy, in 2009 and 2013, respectively. In 2012, he was a Visiting Researcher with The University of Nottingham, U.K. From 2014 to 2017, he was a Postdoctoral Researcher with the University of Kiel, Germany. He is currently an Associate Professor of electrical engineering with the University of Nottingham Ningbo China. He is the author/coauthor of more than 170 scientific papers. His research interests include power electronics for renewable energy systems, smart transformer fed micro-grids, and dc grids for the more electric aircraft.

MARCO LISERRE (S'00–M'02–SM'07–F'13) received the M.Sc. and Ph.D. degrees in electrical engineering from the Bari Polytechnic, in 1998 and 2002, respectively. He has been an Associate Professor with Bari Polytechnic. Since 2012, he has been a professor of reliable power electronics with Aalborg University, Denmark. Since 2013, he has been a Full Professor and holds the Chair of Power Electronics with Kiel University, Germany. He has published 400 technical papers (more than one-third of them in international peer-reviewed journals) and a book. These works have received more than 28 000 citations. He is a member of IAS, PELS, PES, and IES. He has been serving all these societies in different capacities. He was listed in ISI Thomson report "The World's Most Influential Scientific Minds," in 2014. He received the IES 2009 Early Career Award, the IES 2011 Anthony J. Hornfeck Service Award, the 2011 Industrial Electronics Magazine Best Paper Award, and the Third Prize Paper Award by the Industrial Power Converter Committee at ECCE 2012, the 2014 Dr. Bimal Bose Energy Systems Award, the 2017 IEEE PELS Sustainable Energy Systems Technical Achievement Award, and the 2018 IEEE-IES Mittelmann Achievement Award. He received the ERC Consolidator Grant for the project "The Highly Efficient and Reliable Smart Transformer (HEART), a New Heart for the Electric Distribution System."